Chemistry & Biology, Vol. 9, 1043–1049, September, 2002, ©2002 Elsevier Science Ltd. All rights reserved. PII S1074-5521(02)00224-7

Genetic Control by a Metabolite Binding mRNA

Ali Nahvi,[1] Narasimhan Sudarsan,[2] Margaret S. Ebert,[2] Xiang Zou,[3] Kenneth L. Brown,[3] and Ronald R. Breaker[2,4]
[1]Department of Molecular Biophysics and Biochemistry
P.O. Box 208114
[2]Department of Molecular, Cellular and Developmental Biology
P.O. Box 208103
Yale University
New Haven, Connecticut 06520
[3]Department of Chemistry and Biochemistry
Ohio University
Athens, Ohio 45701

Summary

Messenger RNAs are typically thought of as passive carriers of genetic information that are acted upon by protein- or small RNA-regulatory factors and by ribosomes during the process of translation. We report that the 5′-untranslated sequence of the *Escherichia coli btuB* mRNA assumes a more proactive role in metabolic monitoring and genetic control. The mRNA serves as a metabolite-sensing genetic switch by selectively binding coenzyme B_{12} without the need for proteins. This binding event establishes a distinct RNA structure that is likely to be responsible for inhibition of ribosome binding and consequent reduction in synthesis of the cobalamin transport protein BtuB. This finding, along with related observations, supports the hypothesis that metabolic monitoring through RNA-metabolite interactions is a widespread mechanism of genetic control.

Introduction

Living systems make use of a variety of genetic control mechanisms that operate at all levels of the gene expression pathway, ranging from transcription regulation to the modulation of mRNA and protein stability. This mechanistic diversity permits organisms to maintain a complex metabolic state wherein each cell closely monitors its status and that of the surrounding environment. Recognition of biochemical cues is typically achieved by protein receptors and enzymes which modulate their functions in response to changing conditions. In prokaryotes and eukaryotes, a variety of genetic control systems have been identified that involve DNA binding by protein factors [1].

The regulation of gene expression by RNA elements has been largely restricted to mechanisms involving RNA-protein interactions (e.g., see [2] and references therein), antisense interactions [3], transcription attenuation [4], and other related mechanisms [5]. However, it has become evident that RNA has a significant potential for forming complex structural folds, and this potential is currently being exploited by molecular engineers to create RNAs that serve as highly selective receptors for many classes of organic compounds [6, 7]. Furthermore, it has recently been established that the molecular recognition capabilities of RNA can be made to serve as allosteric binding sites for engineered molecular switches, wherein the function of a ribozyme is modulated by the binding of specific effector molecules [8, 9].

Considering these functional characteristics of RNA, several investigators have proposed that direct contact between small organic compounds and natural RNAs might serve as the basis for an undiscovered form of genetic control circuitry [10–14]. Specifically, a binding event between a metabolite and a messenger RNA could bring about structural changes that influence the expression of the RNA without the need for intermediary protein receptors. We were particularly intrigued by recent findings [10] that the 5′-leader sequences of the *btuB* mRNAs of *E. coli* and of *Salmonella typhimurium* have important genetic control structures embedded within them, but that no protein factors have been identified which recognize the coenzyme B_{12} (5′-deoxy-5′-adenosylcobalamin or "AdoCbl") for the purpose of genetic regulation.

We speculated that the *btuB* mRNA leader might indeed be using an allosteric mechanism to control the level of translation in response to the concentration of AdoCbl. Decreased expression of the *btuB* gene, which encodes a transport protein for cobalamin compounds, is observed in cell-based assays when sufficient AdoCbl is present. The mRNA leader could actively participate in reducing the level of protein production by serving as the receptor for AdoCbl recognition and subsequently alter its level of translation. This mechanism would require that the RNA exhibit two essential characteristics of allosteric molecules. First, the RNA must make direct contact with the metabolite in a manner that provides sufficient selectivity to preclude the genetic switch from being triggered by other (perhaps closely related) metabolites. Second, this binding event must stabilize an RNA structure that is distinct from that of the structure formed by the unbound mRNA. This ligand-induced structural modulation would then influence later events such as the efficiency of translation initiation.

Results and Discussion

Metabolite-Induced Structure Modulation of a Messenger RNA

To assess whether the *btuB* leader sequence alone is sufficient for sensing and responding to a metabolite, we employed a molecular probing strategy that relies on the structure-dependent spontaneous cleavage of RNA [15, 16]. The principal mechanism by which an RNA phosphodiester linkage is spontaneously cleaved involves an internal nucleophilic attack by the 2′-oxygen

[4]Correspondence: ronald.breaker@yale.edu

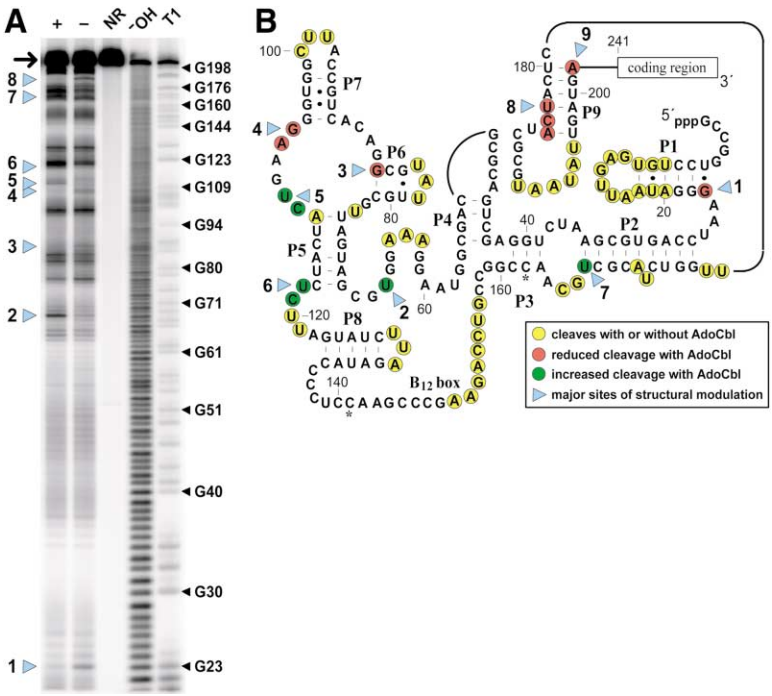

Figure 1. Metabolite-Dependent Conformational Changes in the 202-Nucleotide Leader Sequence of the *btuB* mRNA

(A) Separation of spontaneous RNA-cleavage products of the *btuB* leader using denaturing 10% polyacrylamide gel electrophoresis (PAGE). 5′-^{32}P-labeled mRNA leader molecules (arrow) were incubated for 41 hr at 25°C in 20 mM $MgCl_2$, 50 mM Tris-HCl (pH 8.3 at 25°C) in the presence (+) or absence (−) of 20 μM AdoCbl. Lanes containing RNAs that have undergone no reaction, partial digest with alkali, and partial digest with RNase T1 (G-specific cleavage) are identified by NR, $^{-}$OH, and T1, respectively. The location of product bands corresponding to cleavage after selected guanosine residues are identified by filled arrowheads. Light blue arrowheads labeled 1 through 8 identify eight of the nine locations that exhibit effector-induced structure modulation, which experience an increase or decrease in the rate of spontaneous RNA cleavage. The image was generated using a phosphorimager (Molecular Dynamics), and cleavage yields were quantitated by using ImageQuant software.

(B) Sequence and secondary-structure model for the 202-nucleotide leader sequence of *btuB* mRNA in the presence of AdoCbl. Putative base-paired elements are designated P1 through P9. Complementary nucleotides in the loops of P4 and P9 that have the potential to form a pseudoknot are juxtaposed. Nine specific sites of structure modulation are identified by light blue arrowheads. The asterisks demark the boundaries of the B_{12} box (nucleotides 141–162). The coding region and the 38 nucleotides that reside immediately 5′ of the start codon (nucleotides 241–243) were not included in the 202-nucleotide fragment. The 315-nucleotide fragment includes the 202-nucleotide fragment, the remaining 38 nucleotides of the leader sequence, and the first 75 nucleotides of the coding region.

on the adjacent phosphorus center. Since the precise "in-line" positioning of the 2′-oxygen, phosphorus, and 5′-oxygen atoms of a given RNA linkage is essential for a productive nucleophilic attack to occur [15, 17–20], the rate at which spontaneous cleavage occurs at a given linkage is highly dependent upon the secondary and tertiary structure of the RNA. Specifically, RNA linkages that are formed by nucleotides involved in stable base-paired structures rarely undergo spontaneous cleavage because they rarely adopt an in-line conformation, while nucleotides located in relatively unstructured regions or in certain tertiary-structured regions experience far greater levels of spontaneous cleavage. Thus, probing of an RNA receptor in the absence and presence of its ligand can be used to provide evidence for RNA structural models and even to determine the dissociation constant for a given RNA-ligand interaction [15, 16].

We subjected a preparation of RNAs that encompass nucleotides 1 through 202 of the 5′-untranslated region of the *btuB* mRNA [10, 21] to in-line probing (Figure 1). In the absence of the putative AdoCbl effector, the RNA exhibits a distinct pattern of cleavage products that is indicative of a well-ordered conformational state, which has a mixture of stable structural elements interspersed with regions that are mostly unstructured (Figure 1A). In the presence of AdoCbl, the pattern of cleavage changes at eight locations, while a ninth position of structural modulation (Figure 1B) is observed when a longer portion of the mRNA is used. Specifically, metabolite-induced structural modulation at nucleotide 202 (Figure 1B, position 9) was observed by using in-line probing of a fragment that encompasses nucleotides 1 through 315 of the *btuB* mRNA [10]. Positions 1, 3, 4, 8, and 9 undergo an effector-dependent dampening of spontaneous cleavage, while the remaining sites experience the reverse effect. We also observe a similar pattern of metabolite-modulated RNA cleavage (data not shown) with the analogous 206-nucleotide *btuB* leader RNA of *S. typhimurium* [22].

These effector-modulated sites are mapped on a secondary-structure model that was generated by using a combination of computational and RNA probing data. An RNA secondary-structure prediction algorithm [23] (The Zuker mfold program can be accessed on the internet at http://bioinfo.math.rpi.edu/~mfold/rna/form1.cgi.) supports a model wherein nine base-paired elements are formed. Our in-line probing data and preliminary mutational analyses are consistent with eight of these pairing interactions (P1-P4 and P6-P9), while an alternative pairing interaction (P5) is supported (see below). The majority of these putative base-paired elements appear to remain intact upon effector-induced modulation, with the notable exception of P9. The importance of this structural element in the modulation of ribosome binding and translation has been previously established by mutational analysis [10]. Metabolite-dependent formation of the P9 stem-loop structure appears to be critical for the downregulation of mRNA translation. Consistent with this hypothesis is the observed increase in structure formation in this location upon the addition of AdoCbl (Figure 1B, decreased cleavage at positions 8 and 9).

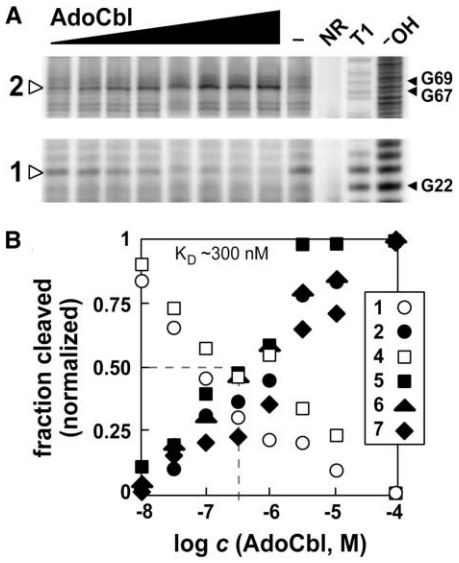

Figure 2. The *btuB* mRNA Leader Forms a Saturable Binding Site for AdoCbl

(A) The dependence of spontaneous cleavage of *btuB* mRNA leader on the concentration of AdoCbl effector as represented by site 1 (G23) and site 2 (U68). 5′-^{32}P-labeled mRNA leader molecules were incubated, separated, and analyzed as described in the legend to Figure 1A, and include identical control and marker lanes as indicated. Incubations contained concentrations of AdoCbl ranging from 10 nM to 100 μM (lanes 1 though 8) or did not include AdoCbl (–).

(B) Composite plot of the fraction of RNA cleaved at six locations along the mRNA leader versus the logarithm of the concentration (*c*) of AdoCbl. Fraction cleaved values were normalized relative to the highest and lowest cleavage values measured for each location, including the values obtained upon incubation in the absence of AdoCbl. The inset defines the symbols used for each of six sites, while the remaining three sites were excluded from the analysis due to weak or obscured cleavage bands. Filled and open symbols represent increasing and decreasing cleavage yields, respectively, upon increasing the concentration of AdoCbl. The dashed line reflects a K_D of ~300 nM, as predicted by the concentration needed to generate half-maximal structural modulation. Data plotted were derived from a single PAGE analysis, of which two representative sections are depicted in (A).

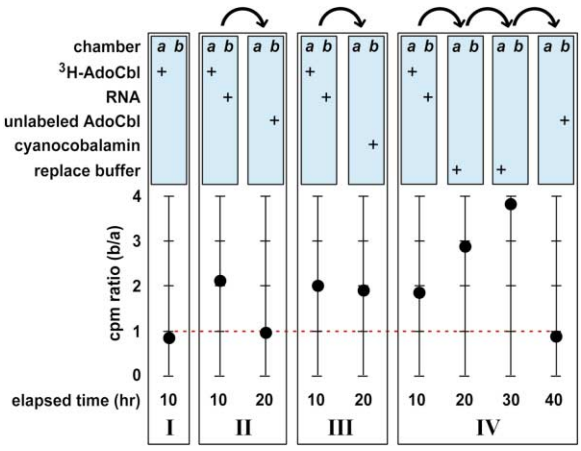

Figure 3. The 202-Nucleotide mRNA Leader Causes an Unequal Distribution of AdoCbl in an Equilibrium Dialysis Apparatus

I, Equilibration of tritiated effector was conducted in the absence of RNA; II (step 1), equilibration was conducted as in I but with 200 pmol of mRNA leader added to chamber *b*, (step 2), 5000 pmol of unlabeled AdoCbl was added to chamber *b*; III, equilibrations were conducted as described in II but 5000 pmol of cyanocobalamin was added to chamber *b*; IV (step 1), equilibration was initiated as described in step 1 of II, (steps 2 and 3), the solution in chamber *a* was replaced with 25 μl of fresh equilibration buffer, (step 4), 5000 pmol of unlabeled AdoCbl was added to chamber *b*. The cpm ratio is the ratio of counts detected in chamber *b* relative to that of *a*. The dashed line represents a cpm ratio of 1, which is expected if equal distribution of tritium is established.

A Saturable Metabolite Binding Site Is Formed by a Messenger RNA

If the structural alteration of the mRNA leader is induced selectively by AdoCbl (as opposed to modulation by a nonspecific effect), then the RNA should exhibit characteristics of a typical receptor-ligand interaction. Thus, a plot of the relative extents of structural modulation at each site is expected to yield an apparent dissociation constant (apparent K_D) for the effector, which reflects the concentration of effector needed to convert half of the RNAs into their altered structural state. Furthermore, if a single binding event brings about the global structural changes that are observed, then the individual K_D values calculated for each modulation site should converge on a single value, while these values are likely to vary if the structural modulation results from nonspecific effects.

Indeed, we find that the levels of spontaneous RNA cleavage correlate with the concentrations of AdoCbl added to the in-line probing mixtures (Figure 2A). Examination of the dependency of the six most prominent sites of modulation on effector concentration reveals similar apparent K_D values of approximately 300 nM at 25°C (Figure 2B). This value is comparable to an apparent K_D value derived from a previous assay that examined the AdoCbl-dependent binding of ribosomes to the *btuB* mRNA [10]. Moreover, the fact that structural modulation occurs over a broad range of concentrations of AdoCbl suggests that this RNA is not likely to make use of cooperative binding of multiple effectors, which would result in a more substantial response to small changes in effector concentration. Together, these observations are consistent with the hypothesis that the mRNA leader undergoes a substantial change in conformation and forms a high-affinity binding pocket for AdoCbl.

To provide further support for this conclusion, we used equilibrium dialysis to determine whether the RNA could selectively generate an unequal distribution of tritiated AdoCbl (^{3}H-AdoCbl) when incubated in a two-chamber dialysis system. As expected, addition of ^{3}H-AdoCbl to chamber *a* of an equilibrium dialysis assembly results in near equal distribution of tritium (cpm ratio ~1) between chambers *a* and *b* upon incubation (Figure 3, experiment I). However, we find that the addition of the 202-nucleotide mRNA leader to chamber *b* causes a shift in the equilibrium of ^{3}H-AdoCbl (cpm ratio ~2) in favor of chamber *b* (Figure 3, experiments II and III). Importantly, we find that the subsequent addition of an excess of unlabeled AdoCbl restores equal distribution of tritium between the two chambers, while the addition of an excess of cyanocobalamin (vitamin B_{12}, an analog

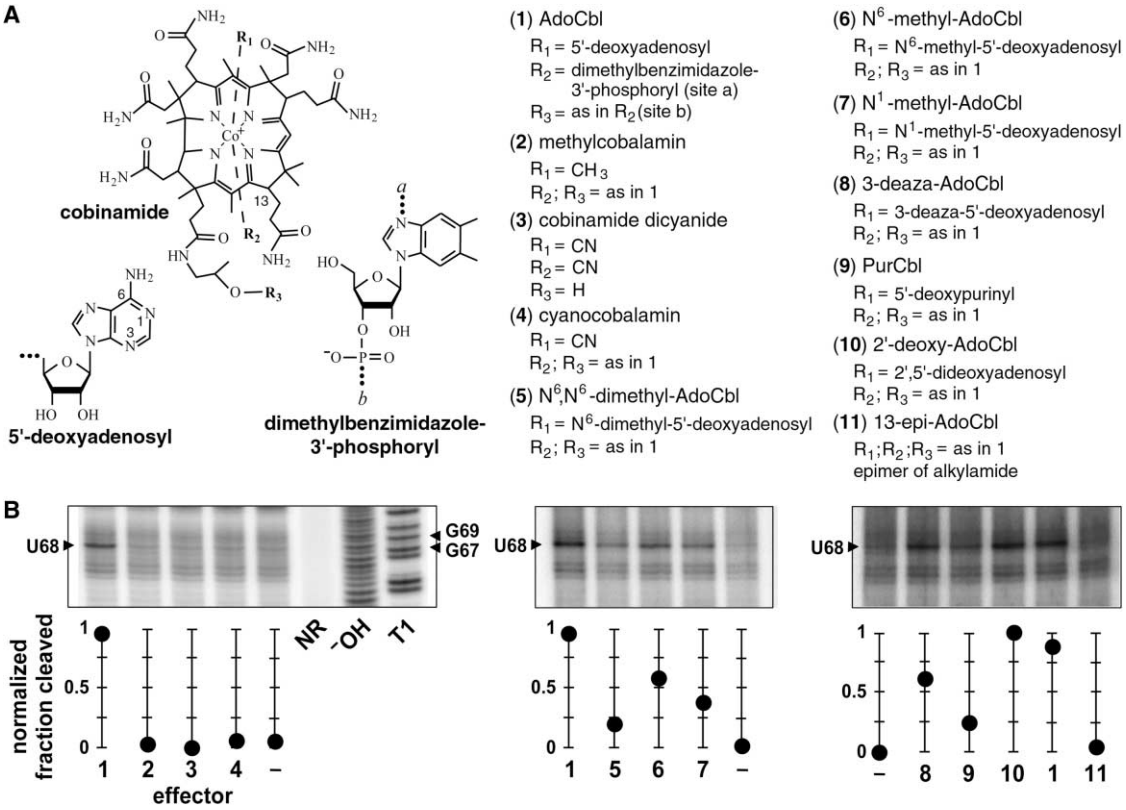

Figure 4. Selective Molecular Recognition of Effectors by the *btuB* mRNA Leader

(A) Chemical structure of AdoCbl (1) and various effector analogs (2–11; [30]).

(B) Determination of analog binding by monitoring modulation of spontaneous cleavage of the 202-nucleotide *btuB* RNA leader. 5′-^{32}P-labeled mRNA leader molecules were incubated, separated, and analyzed as described in the legend to Figure 1A, and include identical control and marker lanes as indicated. The sections of three PAGE analyses encompassing site 2 (U68) are depicted. Below each image is plotted the amount of RNA cleaved (normalized with relation to the lowest and highest levels of cleavage at U68 in each gel) for each effector as indicated or for no effector (−). The compound 11 (13-epi-AdoCbl) is an epimer of AdoCbl wherein the configuration at C13 is inverted so that the *e* propionamide side chain is above the plane of the corrin ring; see [34].

of AdoCbl) does not restore the ratio of tritium to unity. Excess unlabeled AdoCbl is expected to restore equal distribution by serving to occupy the vast majority of the binding sites formed by the *btuB* RNA. In contrast, cyanocobalamin is known to be incapable of serving as a regulatory effector for *btuB* expression in *E. coli* [10, 24] and thus should be ignored as an effector by the RNA. These findings are consistent with the hypothesis that the RNA directly binds AdoCbl and indicate that the RNA forms a selective binding pocket that excludes certain analog compounds.

Assuming that a 1:1 complex is formed between effector and RNA, we had expected that equilibrium dialysis would produce a cpm ratio of far greater than 2 under our assay conditions (2-fold excess RNA over ^{3}H-AdoCbl and concentrations of RNA and effector in excess of the apparent K_D). Since there should be an excess of binding sites, the majority of the tritium should be shifted to chamber *b* upon equilibration. However, our data suggest that ~70% of the tritium in the sample used is not in the form of ^{3}H-AdoCbl. For example, we find that successive replacement of the buffer in chamber *a* (which removes unshifted tritium from the equilibrium dialysis system) results in increasing values for the cpm ratio (Figure 3, experiment IV). In addition, we find that the tritium that remains in chamber *a* upon equilibration with RNA in chamber *b* cannot be induced to yield an unequal distribution of tritium by *btuB* RNA in a subsequent equilibrium dialysis experiment (data not shown). The source of this unbound tritium is most likely from light-mediated degradation of AdoCbl, which is highly unstable under ambient light conditions. Mass spectrum analysis of ^{3}H-AdoCbl reveals that the sample is almost entirely intact in the absence of light exposure but yields ~70% degradation upon exposure to light for a time (~20 s) that is typically experienced by a sample when establishing an equilibrium dialysis experiment.

The *btuB* mRNA Leader Selectively Binds AdoCbl

To provide selectivity for the genetic response, the *btuB* mRNA leader must form a precise binding pocket for AdoCbl in order to preclude the genetic switch from being triggered by other metabolites. To explore the molecular recognition capabilities of this RNA, we indirectly determined the binding affinity of AdoCbl relative to ten analogs (Figure 4A). This was achieved by determining the extent of spontaneous cleavage at site 2 (nucleotide U68) upon incubation in the presence of

AdoCbl or of various analogs (Figure 4B). We find that the RNA fails to undergo structural modulation when cobalamin compounds lack the 5′-deoxy-5′-adenosyl moiety. The importance of individual functional groups on this moiety is revealed by the function of other analogs. In summary, modifications at the N1, N3, and N6 positions of the adenine ring cause significant disruption of binding, while the 2′-hydroxyl group of the adjoining ribose moiety is not an important molecular recognition element. Interestingly, we find that a change in the stereochemistry at position 13 of the corrin ring (compound 11) renders the molecule inactive as a regulatory effector in this in vitro assay and also inside cells (data not shown). These findings indicate that the *btuB* mRNA leader forms a binding pocket for AdoCbl and that the RNA makes numerous contacts with the effector to ensure high molecular specificity.

Disruption of Metabolite-RNA Binding Has Consequences for Genetic Control

The presence of AdoCbl causes reductions in ribosome binding and translation efficiency of the *btuB* mRNA [10]. Our data suggest that this genetic control process is mediated by the selective binding of AdoCbl to the *btuB* mRNA. We compared the effector binding function of mutant RNA leaders in vitro with their ability to support effector-induced genetic control inside cells. As expected, the wild-type mRNA leader exhibits effector-induced structure modulation, induces an unequal distribution of ^{3}H-AdoCbl in an equilibrium dialysis system, and permits downregulation of a reporter gene in *E. coli* cells treated with AdoCbl and harboring the appropriate reporter construct (summarized in Figure 5A). However, the introduction of a single mutation (A150T) in the evolutionarily conserved "B_{12} box" [10] completely eliminates the in vitro effector binding and in vivo gene-control functions of this construct, termed "m1" (Figure 5B), which is consistent with the necessity of effector binding for genetic control.

Using a similar experimental approach, we examined mutations that disrupt (U73G, G74U) and subsequently restore (U73G, G74U, C114A, A115C) the predicted P5 stem element. The disrupted stem in construct m2 causes a reduction of AdoCbl binding affinity in vitro and a corresponding reduction of genetic control in cell assays (Figure 5C), while restoration of the P5 stem element (construct m3) results in near wild-type functions for binding and genetic control (Figure 5D). This suggests that the P5 stem is an important structural element for function of the RNA. Interestingly, potentially disruptive (m4) and restorative (m5) mutations in a possible pseudoknot structure between the P4 and P9 loops (Figure 1B) both result in a reduction in binding affinity ($K_D \sim 5$ μM). If a pseudoknot is being formed, this structure might require a specific sequence for proper function. Although these RNAs maintain diminished but detectable levels of effector binding, neither exhibits genetic control upon the addition of AdoCbl to bacterial cultures harboring the corresponding reporter constructs. We speculate that the loss in binding affinity is sufficient to place these mutant RNAs out of the physiological range for effector concentration, as the cells still retain their

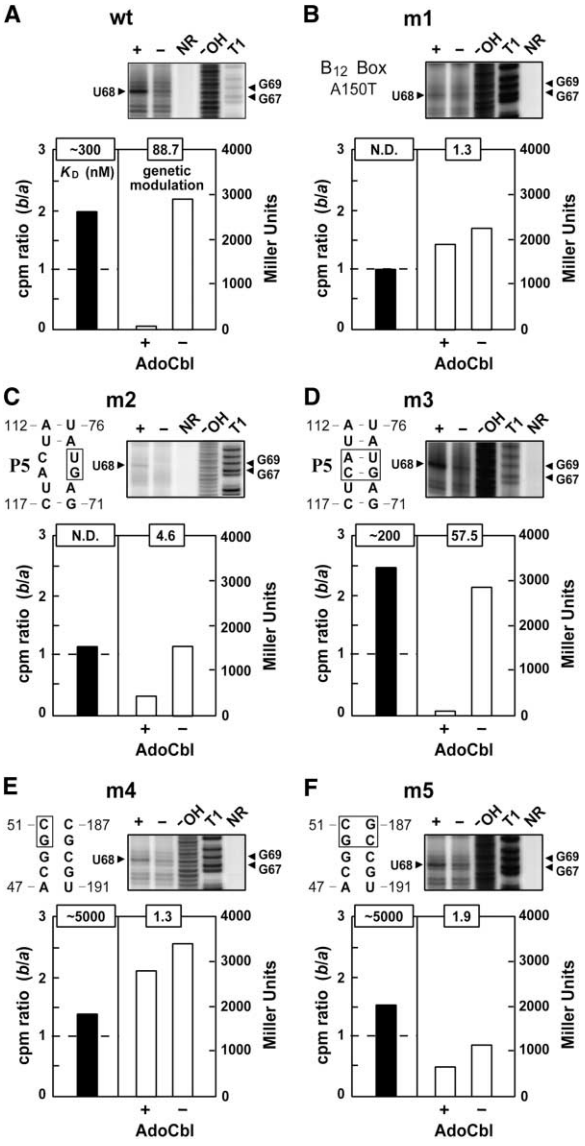

Figure 5. Mutations in the mRNA Leader and Their Effects on AdoCbl Binding and Genetic Control

(A) Sequence of the putative P5 element of the wild-type 202-nucleotide *btuB* leader exhibits AdoCbl-dependent modulation of structure, as indicated by the observed increase in spontaneous RNA cleavage at position U68 (10% denaturing PAGE gel). Assays were conducted in the absence (–) or presence (+) of 5 μM AdoCbl. The remaining lanes are as described in the legend to Figure 1A. The composite bar graph reflects the ability of the RNA to shift the equilibrium of AdoCbl in an equilibrium dialysis apparatus and the ability of a reporter gene (see Experimental Procedures) to be regulated by AdoCbl addition to a bacterial culture. On the left is plotted the cpm ratio derived by equilibrium dialysis, wherein chamber *b* contains the RNA. Details of the equilibrium dialysis experiments are described in the legend to Figure 3. On the right are plotted the expression levels of β-galactosidase as determined from cells grown in the absence (–) or presence (+) of 5 μM AdoCbl. Boxed numbers on the left and right, respectively, reflect the approximate K_D and the fold repression of β-galactosidase activity in the presence of AdoCbl.

(B–F) Sequences and performance characteristics of various mutant leader sequences as indicated. Constructs were created as described in Experimental Procedures. N.D., not determined.

natural *btuB* gene whose regulatory system continues to control the import of AdoCbl. Although many similar experiments need to be performed to confirm the details of the structural model and mechanism of metabolite-induced genetic switching in *btuB* mRNA, our findings support the hypothesis that mRNAs have the structural and functional sophistication needed to perform precision genetic control in the absence of protein regulatory elements.

Significance

Genetic control by mRNAs that directly sense the concentrations of metabolites is a newly established paradigm for monitoring the status of cellular metabolism. Although sensing of aminoacyl tRNAs in prokaryotes also appears to be achieved by direct binding of tRNAs to the 5′-untranslated region of their corresponding aminoacyl tRNA synthetases [25], binding appears to be mediated by Watson/Crick base pairing. In the case of *btuB*, the mRNA directly binds the AdoCbl effector and becomes resistant to translation initiation, presumably by preventing ribosome binding [10]. If no protein receptors are required for molecular recognition or for modulating gene expression, then this simple "riboswitch" mechanism is most economical in its architecture. Given the organizational simplicity of the *btuB* genetic control components compared to analogous systems that involve proteins, it is likely that mRNAs could be more easily engineered to respond directly to natural and nonbiological regulatory effectors. Indeed, examples of engineered mRNAs that mimic the general concept of this natural riboswitch have recently been reported [26, 27].

It is possible that variations of this mechanism involving direct contacts between metabolite and mRNA are far more widespread in genetic circuitry. For example, the *S. typhimurium cob* operon, which encodes proteins in the biosynthetic pathway for the AdoCbl coenzyme, carries B_{12} box and other regulatory structures in its leader domain [28]. We also have data supporting the hypothesis [11, 12] that the "*thi* box" elements found in many mRNAs of genes involved in thiamin metabolism directly bind the coenzyme thiamin pyrophosphate (W. Winkler, A.N., and R.R.B., submitted). It has been noted [29] that these two coenzymes and FMN, which is another potential riboswitch effector [11], possibly are molecular fossils of an ancient metabolic state that was run entirely by RNA. If true, then mechanisms involving metabolite sensing by mRNA might be one of the oldest forms of genetic control in existence.

Experimental Procedures

Chemicals and Oligonucleotides

AdoCbl and its analogs methylcobalamin, cobinamide dicyanide, and cyanocobalamin were purchased from Sigma. Tritiated AdoCbl was prepared as described previously [30]. For information regarding the AdoCbl analogs B^6,N^6-dimethyl-AdoCbl, N^6-methyl-AdoCbl, N^1-methyl-AdoCbl, 3-deaza-AdoCbl, PurCbl, 2′-deoxy-AdoCbl, and 13-epi-AdoCbl, see [31].

DNA oligonucleotides were synthesized by the Keck Foundation Biotechnology Resource Center at Yale University. DNAs were purified by denaturing (8 M urea) PAGE and isolated from the gel by crush/soaking in 10 mM Tris-HCl (pH 7.5 at 23°C), 200 mM NaCl, and 1 mM EDTA. The DNA was recovered from the solution by precipitation with ethanol, resuspended in water, and stored at −20°C until use.

RNA Structure Analysis by In-Line Probing

Precursor mRNA leader molecules were prepared by in vitro transcription from templates generated by PCR (see In Vivo Expression Constructs and Assays section below) and 5′ ^{32}P labeled using methods described previously [8]. Approximately 20 nM of labeled RNA precursor was incubated as described in the legend to Figure 1. Accompanying digestions were carried out using reaction conditions similar to those described previously [15]. To prevent light-induced degradation of ligands, incubations were protected from exposure to light by wrapping each tube with aluminum foil.

Equilibrium Dialysis Assays

Each equilibrium dialysis experiment was conducted using a Dispo-Equilibium Dialyzer (ED-1, Harvard Bioscience) apparatus, wherein two chambers (*a* and *b*) each contained 25 μl of equilibration buffer (50 mM Tris-HCl [pH 8.3 at 25°C], 20 mM $MgCl_2$). The chambers were separated by a dialysis membrane with a 5000 Da molecular weight cut-off. In each experiment (Figure 3, I–IV, boxed), 100 pmol of ^{3}H-AdoCbl was included in chamber *a*, and other additives were included as designated (+) for each chamber. In each step, equilibrations were allowed to proceed for 10 hr at 25°C before samples were quantitated or before subsequent manipulations were carried out. Quantitation was achieved by liquid scintillation counting using 5 or 10 μl of solution from each chamber. Dialysis samples were protected from exposure to light by wrapping each apparatus with aluminum foil.

In Vivo Expression Constructs and Assays

E. coli K-12 strain was used for all *btuB-lacZ* expression assays, and Top10 cells (Invitrogen) were used for plasmid preparation. A DNA (nucleotides –70 to 450) encompassing the *btuB* leader sequence was amplified as an EcoRI-BamHI fragment by colony PCR from *E. coli* strain MC4100 (a gift from S. Gottesman, NIH). The wild-type construct and mutant constructs were inserted into plasmid pRS414 (a gift from R. Simons, UCLA; [32]) in frame with the ninth codon of *lacZ* (β-galactosidase). Mutant constructs were generated by a three-step PCR strategy wherein regions upstream and downstream of the mutation site were amplified separately with the appropriate DNA primers that introduced the desired sequence changes. The resulting fragments were purified by agarose gel electrophoresis and then combined and amplified by PCR using primers that correspond to the ends of the full-length construct. The resulting constructs were cloned and sequenced. Constructs whose sequence was confirmed were used for expression analysis and were used as templates for subsequent preparation of PCR-derived DNAs for in vitro transcription.

The in-frame fusions between various *btuB* leader sequences and *lacZ* generated as described above were used to determine the levels of expression by employing a β-galactosidase assay adapted from that described by Miller [33].

Acknowledgments

We thank members of the Breaker laboratory for helpful discussions. We also thank J. McKinney and S. Altman for a sample of *S. typhimurium* genomic DNA and A. Miranker for assistance with mass spectroscopy. This work was supported by NIH grants to K.L.B (GM 48858) and to R.R.B (GM 559343) and by an NSF grant (EIA-0129939) to R.R.B. M.S.E is supported by the Beckman Scholars Program for undergraduate research, which is sponsored by the Arnold and Mabel Beckman Foundation. RNA science in the Breaker laboratory also is supported through a fellowship to R.R.B. from the David and Lucile Packard Foundation.

Received: August 21, 2002
Revised: September 4, 2002
Accepted: September 4, 2002

References

1. Struhl, K. (1999). Fundamentally different logic of gene regulation in eukaryotes and prokaryotes. Cell *98*, 1–4.
2. Henkin, T.M. (1996). Control of transcription termination in prokaryotes. 1996. Annu. Rev. Genet. *30*, 35–57.
3. Simons, R.W., and Wagner, E.G. (1994). Antisense RNA control in bacteria, phages, and plasmids. Annu. Rev. Microbiol. *48*, 713–742.
4. Landick, R., Turnbough, C.L., Jr., and Yanofsky, C. (1996). Transcription attenuation. In Escherichia coli and Salmonella, F.C. Neidhardt, et al., eds. (Washington, D.C.: American Society for Microbiology Press), pp. 1263–1286.
5. Szymański, M., and Barciszewski, J. (2002). Beyond the proteome: non-coding regulatory RNAs. Genome Biol. Published online April 15, 2002. reviews0005.1-0005.8, http://genomebiology.com/2002/3/5/reviews/0005.
6. Famulok, M. (1999). Oligonucleotide aptamers that recognize small molecules. Curr. Opin. Struct. Biol. *9*, 324–329.
7. Hermann, T., and Patel, D.J. (2000). Adaptive recognition by nucleic acid aptamers. Science *287*, 820–825.
8. Soukup, G.A., and Breaker, R.R. (2000). Allosteric nucleic acid catalysts. Curr. Opin. Struct. Biol. *10*, 318–325.
9. Seetharaman, S., Zivarts, M., Sudarsan, N., and Breaker, R.R. (2001). Immobilized RNA switches for the analysis of complex chemical and biological mixtures. Nat. Biotechnol. *19*, 336–341.
10. Nou, X., and Kadner, R.J. (2000). Adenosylcobalamin inhibits ribosome binding to *btuB* RNA. Proc. Natl. Acad. Sci. USA *97*, 7190–7195.
11. Gelfand, M.S., Mironov, A.A., Jomantas, J., Kozlov, Y.I., and Perumov, D.A. (1999). A conserved RNA structure element involved in the regulation of bacterial riboflavin synthesis genes. Trends Genet. *15*, 439–442.
12. Miranda-Rios, J., Navarro, M., and Soberón, M. (2001). A conserved RNA structure (*thi* box) is involved in regulation of thiamin biosynthetic gene expression in bacteria. Proc. Natl. Acad. Sci. USA *98*, 9736–9741.
13. Stormo, G.D., and Ji, Y. (2001). Do mRNAs act as direct sensors of small molecules to control their expression? Proc. Natl. Acad. Sci. USA *98*, 9465–9467.
14. Gold, L., Brown, D., He, Y., Shtatland, T., Singer, B.S., and Wu, Y. (1997). From oligonucleotide shapes to genomic SELEX: Novel biological regulatory loops. Proc. Natl. Acad. Sci. USA *94*, 59–64.
15. Soukup, G.A., and Breaker, R.R. (1999). Relationship between internucleotide linkage geometry and the stability of RNA. RNA *5*, 1308–1325.
16. Soukup, G.A., DeRose, E.C., Koizumi, M., and Breaker, R.R. (2001). Generating new ligand-binding RNAs by affinity maturation and disintegration of allosteric ribozymes. RNA *7*, 524–536.
17. Westheimer, F.H. (1968). Pseudo-rotation in the hydrolysis of phosphate esters. Acc. Chem. Res. *1*, 70–78.
18. Usher, D.A. (1969). On the mechanism of ribonuclease action. Proc. Natl. Acad. Sci. USA *62*, 661–667.
19. Usher, D.A., and McHale, A.H. (1976). Hydrolytic stability of helical RNA: a selective advantage for the natural 3′,5′-bond. Proc. Natl. Acad. Sci. USA *73*, 1149–1153.
20. Dock-Bregeon, A.C., and Moras, D. (1987). Conformational changes and dynamics of tRNAs: evidence from hydrolysis patterns. Cold Spring Harb. Symp. Quant. Biol. *52*, 113–121.
21. Lundrigan, M.D., Köster, W., and Kadner, R.J. (1991). Transcribed sequences of the *Escherichia coli* btuB gene control its expression and regulation by vitamin B_{12}. Proc. Natl. Acad. Sci. USA *88*, 1479–1483.
22. Wei, B.Y., Bradbeer, C., and Kadner, R.J. (1992). Conserved structural and regulatory regions in the Salmonella typhimurium btuB gene for the outer membrane vitamin B12 transport protein. Res. Microbiol. *143*, 459–466.
23. Zuker, M., Mathews, D.H., and Turner, D.H. (1999). Algorithms and thermodynamics for RNA secondary structure prediction: a practical guide. In RNA Biochemistry and Biotechnology, J. Barciszewski and B.F.C. Clark, eds. (NATO ASI Series: Kluwer Academic Publishers), pp. 11–43.
24. Lundrigan, M.D., and Kadner, R.J. (1989). Altered cobalamin metabolism in Escherichia coli btuR mutants affects btuB gene regulation. J. Bacteriol. *171*, 154–161.
25. Henkin, T.M. (1994). tRNA-directed transcription antitermination. Mol. Microbiol. *3*, 381–387.
26. Werstuck, G., and Green, M.R. (1998). Controlling gene expression in living cells through small molecule-RNA interactions. Science *282*, 296–298.
27. Harvey, I., Garneau, P., and Pelletier, J. (2002). Inhibition of translation by RNA–small molecule interactions. RNA *8*, 452–463.
28. Ravnum, S., and Andersson, D.I. (2001). An adenosyl-cobalamin (coenzyme-B_{12})-repressed translational enhancer in the *cob* mRNA of *Salmonella typhimurium*. Mol. Microbiol. *39*, 1585–1594.
29. White, H.B., III. (1976). Coenzymes as fossils of an earlier metabolic state. J. Mol. Evol. *7*, 101–104.
30. Brown, K.L., and Zou, X. (1999). Thermolysis of coenzymes B_{12} at physiological temperatures: activation parameters for cobaltcarbon bond homolysis and a quantitative analysis of the perturbation of the homolysis equilibrium by the ribonucleoside triphosphate reductase from *Lactobacillus leichmannii*. J. Inorg. Biochem. *77*, 185–195.
31. Toraya, T. (1999). Diol dehydratase and glycerol dehydratase. In Chemistry and Biochemistry of B_{12}, R. Banerjee, ed. (New York: Wiley), pp. 783–809.
32. Simons, R.W., Houman, F., and Kleckner, N. (1987). Improved single and multicopy lac-based cloning vectors for protein and operon fusions. Gene *53*, 85–96.
33. Miller, J.H. (1992). Procedures for working with *lac*. In A Short Course in Bacterial Genetics. (Cold Spring Harbor, NY: Cold Spring Harbor Laboratory Press) p. 72.
34. Brown, K.L., Cheng, S., and Marques, H.M. (1998). Conformational studies of 5′-deoxyadenosyl-13-epicobalamin, a coenzymatically active structural analog of coenzyme B_{12}. Polyhedron *17*, 2213.